Enhancemet of flow boiling heat transfer in pHEMA/pPFDA coated microtubes with longitudinal variations in wettability

Cite as: AIP Advances **6**, 035212 (2016); https://doi.org/10.1063/1.4944581
Submitted: 09 December 2015 • Accepted: 02 March 2016 • Published Online: 15 March 2016

Masoumeh Nedaei, Efe Armagan, Meltem Sezen, et al.

Enhancemet of flow boiling heat transfer in pHEMA/pPFDA coated microtubes with longitudinal variations in wettability

Masoumeh Nedaei,[1] Efe Armagan,[2] Meltem Sezen,[3] Gozde Ozaydin Ince,[2] and Ali Kosar[1,a]

[1]*Mechatronics Engineering Program, Faculty of Engineering and Natural Sciences, Sabanci University, Istanbul 34956, Turkey*
[2]*Materials Science and Nanoengineering Program, Faculty of Engineering and Natural Sciences, Sabanci University, Tuzla, Istanbul 34956, Turkey*
[3]*Nanotechnology Research and Application Center (SUNUM), Sabanci University, Tuzla, 34956 Istanbul, Turkey*

(Received 9 December 2015; accepted 2 March 2016; published online 15 March 2016)

Flow boiling heat transfer was investigated in stainless steel hypodermic microtubes, whose surfaces were enhanced by gradient crosslinked polyhydroxyethylmethacrylate (pHEMA)/polyperfluorodecylacrylate (pPFDA) coatings thereby offering variations in wettability along the surface as well as high porosity. The initiated chemical vapor deposition (iCVD) method was implemented for coating the inner walls of the microtubes with an inner diameter of 502 μm, and deionized water was used as the working fluid. Experimental results were obtained from the coated microtubes, where one end corresponded to the pHEMA (hydrophilic) coated part and the other end was the most hydrophobic location with the pPFDA (hydrophobic) coating so that wettability varied along the length of the microtube. The results of both the hydrophobic and hydrophilic inlet cases were compared to their plain surface counterparts at the mass flux of 9500 kg/m^{2}s. The experimental results showed a remarkable increase in boiling heat transfer with the coatings. The highest heat transfer coefficients were attained for the pHEMA coated (hydrophobic inlet and hydrophilic outlet) outlet case with a maximum heat transfer enhancement ratio of ~64%. The reason for the enhanced heat transfer with the coated microtubes can be attributed to the increased nucleation site density and bubble release as well as enhanced convection and bubble motion near the surface due to the variation in wettability along the length. The results proved that gradient pHEMA/pPFDA coatings can be utilized as a viable surface enhancement method in microscale cooling applications. [http://dx.doi.org/10.1063/1.4944581]

I. INTRODUCTION

High heat flux cooling is one of the most urgent needs in the thermal-fluid science community and has a broad range of applications in microelectronics,[1] fuel cells,[2–4] nuclear reactors,[5] aerospace applications,[6] bioengineering,[1,7] and drug delivery.[8] Boiling heat transfer has been considered as a promising method for reaching high heat removal rates and has been extensively investigated.[9–14] In the literature, many studies have been conducted to enhance boiling heat transfer via surface modifications.[15–36]

For example, Frost and Kipperhan[15] utilized water with and without different concentrations of surfactant "Ultra Wet 60L" to investigate boiling heat transfer in a vertical annulus. They observed

[a]Corresponding author, Tel: (+90)216-4839621, Fax: (+90)216-4839550, E-mail: kosara@sabanciuniv.edu

an increase in heat transfer rate, which was linked to a reduction in the surface tension. Gulliksen et al.[16] studied boiling heat transfer performance of porous coatings for possible applications in electronics cooling. They observed a reduction in superheat incipience as well as an increase in the heat transfer coefficient compared to the polished Silicon surfaces. Wen and Wang[17] performed their experiments using deionized water and acetone with different surfactants including 95% sodium dodecyl sulfate (SDS), Triton X-100 and octadecylamine on both smooth and roughened surfaces to highlight the influence of fluid wettability on nucleate pool boiling. Emery papers with different grits were used to grind both smooth and roughened surfaces. They found that the roughened surfaces could improve boiling heat transfer with Triton X-100 solutions due to the increased nucleation site density. Sarwar et al.[18] tested different aluminium porous coatings inside a tube at mass fluxes between 100 and 300 kg/m^{2}s and subcoolings of 50°C and 75°C. The results showed that Al_2O_3 coatings offered higher heat transfer coefficients (HTC) than TiO_2 coatings.

Phan et el.[19,20] studied the effects of surface wettability on heat transfer characteristics. They coated a single rectangular channel having a height of 0.5 mm, a width of 5 mm and a length of 180 mm with silicon oxide (SiO_x), titanium (Ti), diamond like-carbon (DLC), and carbon-doped silicon oxide (SiOC) coatings, whose static contact angles were 24 °, 49 °, 63 °, and 104 °, respectively. The experiments performed at the mass flux of 100 kg/m^{2}s illustrated that extended boiling curves (implying higher critical heat fluxes) belonged to the surfaces with lower static contact angles. They also utilized nanostructure coatings to change the water contact angle during subcooled pool boiling. The experimental results revealed an increase in HTC with the highest heat transfer coefficient corresponding to the contact angles close to 0° or 90°. Khanikar et al.[21] coated rectangular microchannels with carbon nanotubes (CNTs) to study flow boiling. Extended boiling curves could be obtained using CNTs compared to plain surfaces. However, repetitions of the tests altered the morphology of CNTs and reduced CHF enhancement. Similar results were recently obtained by Kumar et al.,[22] who employed CNTs and diamond coatings in a minichannel ($25 \times 20 \times 0.4$ mm).

Forrest et al.[23] utilized silica nanoparticle thin-film coatings on nickel wires to study pool boiling heat transfer. The experimental results showed enhancements up to ~100% (corresponding to the hydrophobic surface). Wu et al.[24] investigated boiling of water and FC-72 on hydrophilic titanium oxide (TiO_2) and silicon oxide (SiO_2) modified surfaces, which had about the same roughnesses. The experiments at high heat fluxes in FC-72 tests demonstrated that enhancements up to ~45.6% and ~91.2% were obtained from SiO_2 and TiO_2 coated surfaces, respectively. Such enhancements were attributed to the reduced dry patches due to more liquid-solid interactions of such hydrophilic surfaces. Krishnamurthy and Peles[25] investigated subcooled and low quality saturated flow boiling in a microchannel containing micro pin fins at different mass fluxes and heat fluxes. The heat transfer performance was significantly improved with pin fins.

Stutz et al.[26] utilized nanoparticle coatings on a 100 μm diameter platinum wire for two types of fluids including water and pentane. Nanoparticle deposition was observed using ionic nanoparticles (γ-Fe_2O_3) with an average diameter of 10 nm in two ways: vigorous boiling and electrophoresis. The results showed a poor heat transfer performance for wires, which were wholly covered with nanoparticles. Jo et al.[27] investigated nucleate boiling heat transfer on hydrophobic, hydrophilic and heterogeneous surfaces. They prepared hydrophobic dots on a hydrophilic surface thereby offering a heterogeneous surface. Their findings showed higher heat transfer coefficients on heterogeneous surfaces, while hydrophobic surfaces offered higher HTC at low heat fluxes compared to hydrophilic surfaces. Morshed et al.[28] utilized copper nanowire coatings (CuNWs) in a microchannel having a hydraulic diameter of 672 μm. Boiling heat transfer enhancement of ~56% was accomplished with CuNWs coated microchannels. Kaya et al.[29] utilized crosslinked polyhydroxyethylmethacrylate (pHEMA) coatings on inner microtube walls (with inner diameters of 249 μm, 507 μm, and 908 μm) to investigate heat transfer performance at two mass fluxes of 10,000 and 13,000 kg/m^{2}s. They obtained a maximum increase of 109% in heat transfer coefficient from the microtube configuration of the smallest size. Cikim et al.[30] investigated pHEMA coatings at different thicknesses (50 nm, 100 nm, and 150 nm) and mass fluxes of 5000 kg/m^{2}s and 20000 kg/m^{2}s. They observed a more superior heat transfer performance for larger coating thicknesses.

Morshed et al.[31] performed flow boiling experiments on a microchannel with a hydraulic diameter of 672 μm by depositing Al_2O_3 nanoparticles on the surface. CHF was enhanced for the

modified surfaces by 39%, while degradation in HTC was observed on the coated surfaces. Morshed et al.[32] utilized Cu-Al_2O_3 nanocomposite coatings on the bottom surface of the same microchannels using the electrodeposition technique. The obtained heat transfer enhancements were in the range of 30%-120%. Ji et al.[33] examined pool boiling on different types of heaters having plain, open channel, uniform porous coating and 2D/3D porous coatings with acetone as the working fluid. The results exhibited significant heat transfer enhancements for 2-D/3-D porous coating surfaces.

In the study of Betz et al.,[34] surfaces with different wettabilities (including hydrophilic, hydrophobic, superhydrophobic, superhydrophilic, biphilic and superbiphilic) were tested in pool boiling experiments. The largest heat transfer enhancement was achieved on superbiphilic surfaces with HTC more than 150 kW/ m^2K. Bai et al.[35] studied flow boiling heat transfer in microchannels with metallic porous coatings, which were prepared using the solid state sintering technique. They compared their results with those of a bare surface microchannel. Anhydrous ethanol was utilized as the test fluid. Coated microchannels demonstrated a substantial increase in HTC. They also noticed that heat transfer was more enhanced at lower vapor qualities owing to more nucleation site density. Kumar et al.[36] accomplished spray pyrolyzed Fe doped Al_2O_3-TiO_2 composite coatings in a mini channel (30 mm × 20 mm × 0.4 mm) to study flow boiling heat transfer enhancements at two mass fluxes of 88 and 248 kg/m^2s. They reported a maximum HTC enhancement of 44.1 % corresponding to 7.2% Fe doped Al_2O_3-TiO_2 at the mass flux of 88 kg/m^2s, which was related to its high porosity.

From the abovementioned studies, it can be realized that micro/nano structured surfaces as well as nanofilm deposition on different surfaces have been considered as an effective method to augment boiling heat transfer. Motivated from such studies, polyhydroxyethylmethacrylate (pHEMA) and polyperfluorodecylacrylate (pPFDA) coatings, which provide variations in wettability along the surface as well as high porosity, were applied to the inner walls of microtubes for flow boiling heat transfer enhancement in such a way that nucleation from the tube walls was more likely to occur at specific locations of the microtube. Accordingly, nucleation occurs at a more upstream location in the hydrophobic inlet (pPFDA coating at the inlet and pHEMA coating at the outlet) configuration compared to the hydrophobic outlet (pHEMA coating at the inlet and pPFDA coating at the outlet). SEM (Scanning Electron Microscopy) secondary electron (SE) images of the coated microtubes were also acquried using a JEOL JIB 4601F MultiBeam platform (shown in Fig. 1). The figure shows the overall shape of the tubes, surface morphology and the inner side of the coated tubes. The images were obtained at 5 keV electron energy for different magnifications from the same microtube. Flow boiling heat transfer experiments were performed on microtubes having the same inner diameter of 502 μm with appropriate coatings at the high mass flux of 9500 kg/m^2s. Initiated chemical vapor deposition (iCVD) method was implemented as the deposition method due to its efficiency, rather low cost, and simplicity. Moreover, iCVD can be applicable to any cross section area geometry including closed geometries such as round channels, where standard microfabrication methods such as lithography and etching cannot be implemented.

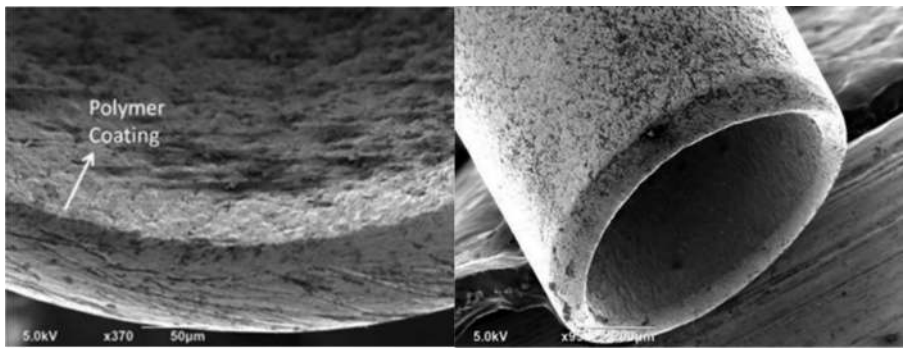

FIG. 1. SEM images of the coated microtubes.

II. EXPERIMENTAL DESCRIPTION

A. Gradient coating deposition methodology

Polymer thin film deposition onto complex geometries, such as micro/nano channels or porous structures, is a very problematic task. Conventional solution based polymerization techniques are not able to coat polymer on all edges of these structures due to the liquid surface tension and wetting effect. However, vapor deposition techniques enable the deposition of polymer thin films with reasonable conformality and high purity which are necessary for polymeric microchannel applications. Uniform coating of metallic microtubes with an inner diameter of 502 μm is a very challenging task via solution based polymerization methods. Besides, solution techniques can leave many residuals behind, which decrease the uniformity of the coating and microchannel's performance. Thus, initiated chemical vapor deposition (iCVD) technique is proposed to deposit gradient poly (hydroxyethyl methacrylate) p (HEMA)/ poly (perfluorodecylacrylate) p (PFDA) into metal microtubes in order to enhance conformality and homogeneity. Due to being solventless and one step process of iCVD, it is possible to coat very complex geometries. Furthermore, iCVD technique compared to other techniques provides depositing polymer on delicate substrates that results in polymeric thin films with good purity.[37]

iCVD is a type of hot wire chemical vapor deposition technique (HWCVD) whose crucial advantages were proven in many studies.[37–39] Free radical polymerization, which is composed of three steps, initiation, propagation and termination, takes place in the iCVD technique as shown in Fig. 2.[37] The monomer, which is heated to a certain temperature in order to obtain enough vapor pressure, and initiator molecules are delivered into the chamber simultaneously. Firstly, the initiator is decomposed into radical molecules by heated filaments. The heated monomers are directly adsorbed by the cool stage without any decomposition. The radical molecules then attack the C=C bonds of the monomers, initiating the polymerization, and continuous delivery of the monomer molecules to the surface enables propagation reactions. There are many kinetic studies on experimental parameters of iCVD, which can be tuned to obtain enhancement in the film composition, conformality, and growth rate, such as chamber pressure, monomer/initiator flowrate, substrate temperature, and filament

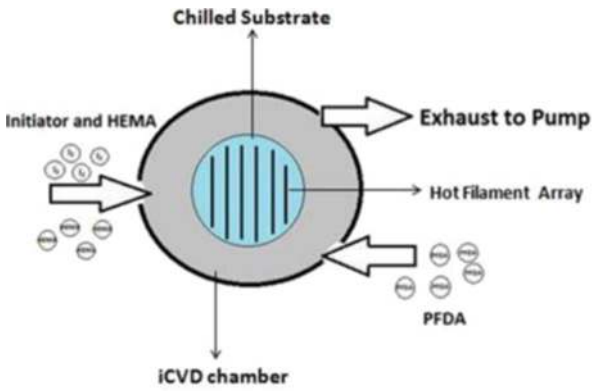

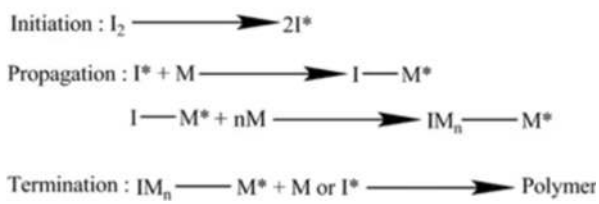

FIG. 2. A radical molecule formation, polymer growth, and polymerization in iCVD method including three main steps, initiation, propagation and termination.

temperature.[40] Gradient deposition was achieved by delivering the HEMA and PFDA monomers to the chamber from the opposite directions so that the HEMA/PFDA ratio of the polymer gradually increased from one end to the other. The flowrate of HEMA and PFDA monomers were respectively set to 0.9 and 0.3 sccm, while the ethylene glycoldimethacrylate (EGDMA) (as a crosslinker) flow rate was 0.08 sccm. During iCVD, the substrate and filament temperatures were kept at 25 °C and 250 °C. The chamber pressure was maintained at 300 mTorr. All depositions for microtubes with diameters of 502 μm were carried out for 30 minutes in order to obtain 150 nm thick films on bare Si wafer.

B. Complementary Analysis

1. Raman Spectroscopy

Raman spectroscopy is commonly used to obtain fingerprint of the identified molecules in a sample. A laser light used in Raman scattering interacts with excitations in the sample and provides up or down shifts in the energy of laser photons. Raman spectroscopy method was utilized to analyse gradient pHEMA/pPFDA coatings. Raman spectral analysis was performed at the Renishaw in Via Raman microscope with laser and grating specifications of a 532 nm and 2400 lines/mm, respectively. The measurements revelaed the differences in chemistry of the polymer thin films.

Figure 3 shows the comparative Raman spectra of pPFDA and pHEMA layers in the coated tubes. The large band around 2950 cm^{-1} corresponds to the $\nu_{as}CH_2$ stretching mode.[41] It has been reported that the high region between 2800 and 3100 cm^{-1} includes the Raman bands that are due to valence vibrations of CH_2 and CH_3.[29] The Raman band at 1454 cm^{-1} demonstrates the deformation of C–H group. The C=C bonds are expected to be deformed during the synthesis process due to the fact that the polymer coatings were deposited inside the tubes by means of free radial polymerization. The band at 1648 cm^{-1} can be attributed to the C=C stretching mode of pPFDA coating. The Raman bands at 1725 and 1740 cm^{-1} correspond to νC=O vibration mode for pHEMA and pPFDA thin film coatings, respectively. (ν: stretching, s: symmetric, as: asymmetric).[41]

In addition, it should be noticed that the band at 2330 cm^{-1} is a noise peak originating from the humid testing environment, not from the samples. It is also found that after performing boiling experiments, there has been no significant change in Raman results for both of the polymer coatings.

2. Energy Dispersive Spectra Measurements

Energy Dispersive Spectra (EDS) measurements were used to detect the elemental distribution and chemical characterization of the polymer thin film coatings. As can be observed from

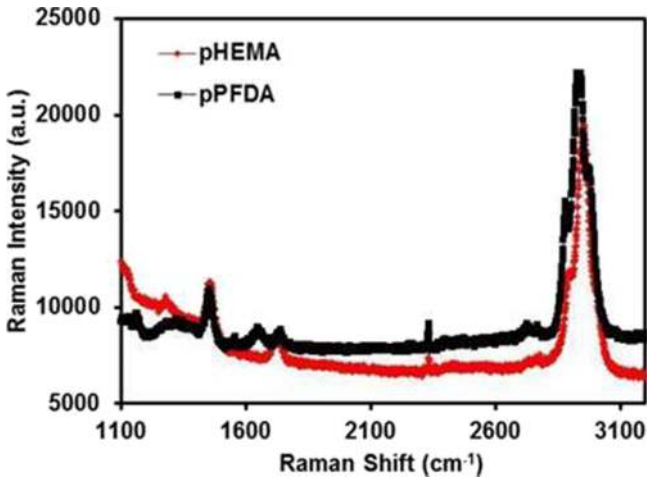

FIG. 3. Raman spectrum taken from the inner surface of the coated microtubes.

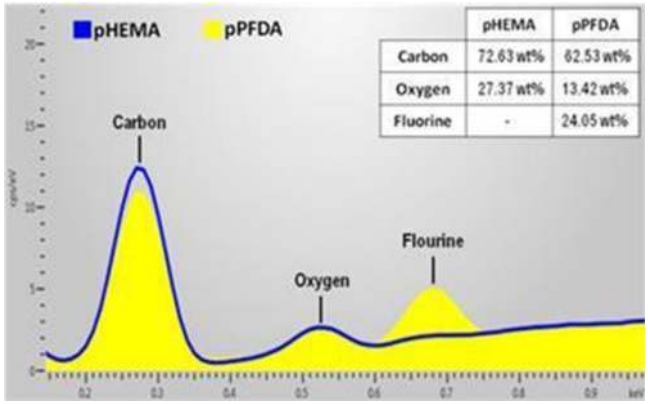

FIG. 4. Energy dispersive spectra measurements of the coated microtubes.

Fig. 4, the pHEMA coated part of the microtubes only contains carbon (72.63 wt. %) and oxygen (27.37 wt. %), while pPFDA includes carbon (62.53 wt. %), oxygen (13.42 wt. %) and fluorine (24.05 wt. %). EDS analyses were performed at the Oxford EDS Xmax- N system, which is coupled to the JEOL JIB 4601F MultiBeam platform, using 15keV electron energy and around 30% dead time for signal acquisition.

3. Contact Angle Measurements

Contact angle measurements were conducted to investigate the hydrophilicity of the surface for different HEMA/PFDA ratios. For these measurements, Si wafers, which were placed next to the microtubes and were coated simultaneously with the same polymer, were used. Figure 5 shows contact angles as a function of the position on Si wafer. It is observed that as going towards the hydrophobic side, the contact angle increases up to 109°, while it reduces to 43° as approaching to the hydrophilic side, confirming the gradient composition of the polymer coating. In the literature, the contact angles of pure pHEMA and pure pPFDA were measured as 37° and 120.8°, respectively.[42,43] The contact angles obtained in this study are within the range reported in the literature.

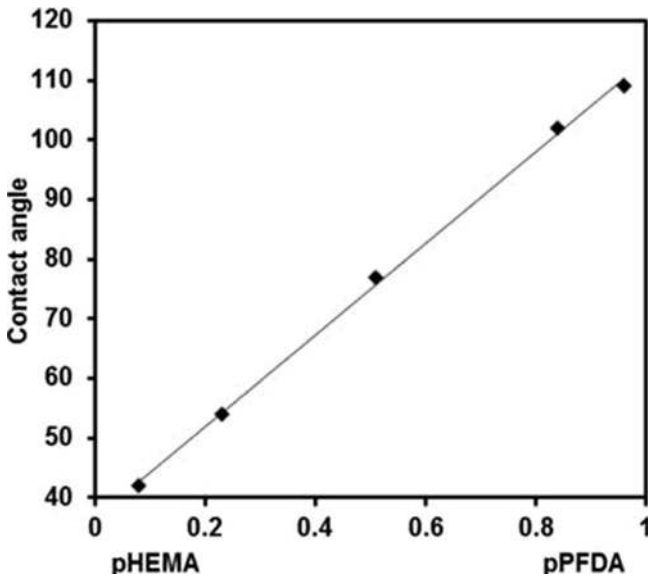

FIG. 5. Contact angles between water droplet and coated surface versus position (location/length of the channel).

C. Experimental Apparatus and Procedure

The schematic of the experimental setup is shown in Fig. 6. It consisted of a storage cylinder, an Omega® flow meter, a Xantrex XFR2800 power supply, Omega® pressure sensors, thermocouples, a water filter, test section and proper tubing and fittings. De-ionized (DI) water was used as the working fluid in the experiments. Pressurized Nitrogen gas was utilized for pumping the working fluid from the reservoir. A filter of 15 μm sieve diameter was utilized. Two alligator clips, specially shaped with machining tools in order to minimize the heated length and to reach a width of 1 mm, were connected to the microtube surface while adjusting the heated length. The heated length was fixed at 2 cm during the experiments. The high current power supply with an adjustable DC current and high power input provides heating along the heated length to provide the desired heat flux to the prescribed sections of 6 cm long microtubes with inner diameters of 502 μm. The inlet side of the microtube was connected to the setup, while the outlet side was exposed to the atmosphere to attain atmospheric conditions at the exit. One Omega® thermocouple was installed upstream the inlet to measure bulk fluid temperatures at the inlet. Multiple Omega® pressure transducers having different ranges of 0-3000 psi gauge pressure were utilized for pressure measurements. The flow rate data obtained from an Omega® turbinemeter were collected together with the current and voltage data. A thin Omega® thermocouple wire (~76 μm) was carefully attached on the microtube surface at the desired location via Omega® Bond just at the outlet, where the maximum temperature was expected at the test section, to measure the local surface temperature at the outlet of the tube. During the experiments, the flow rate was fixed at the desired value by regulating the pressure difference between the microtube inlet and exit. Pressure and temperature data were acquired via the Labview® interface after reaching steady state conditions.

Heat losses were assessed by applying power to the test section after evacuating the test section until the temperature of the test section reaches the steady state value. Thereafter, the temperature difference between the test section and ambient was recorded with the corresponding power value so that power against temperature rise profile was obtained. Thus, the heat loss associated with each experimental data point was found with the use of the resulting calibration curve. Accordingly, heat losses were estimated to be about 6% on average. This amount of heat loss is not very significant as expected due to the high flow rates in this study.

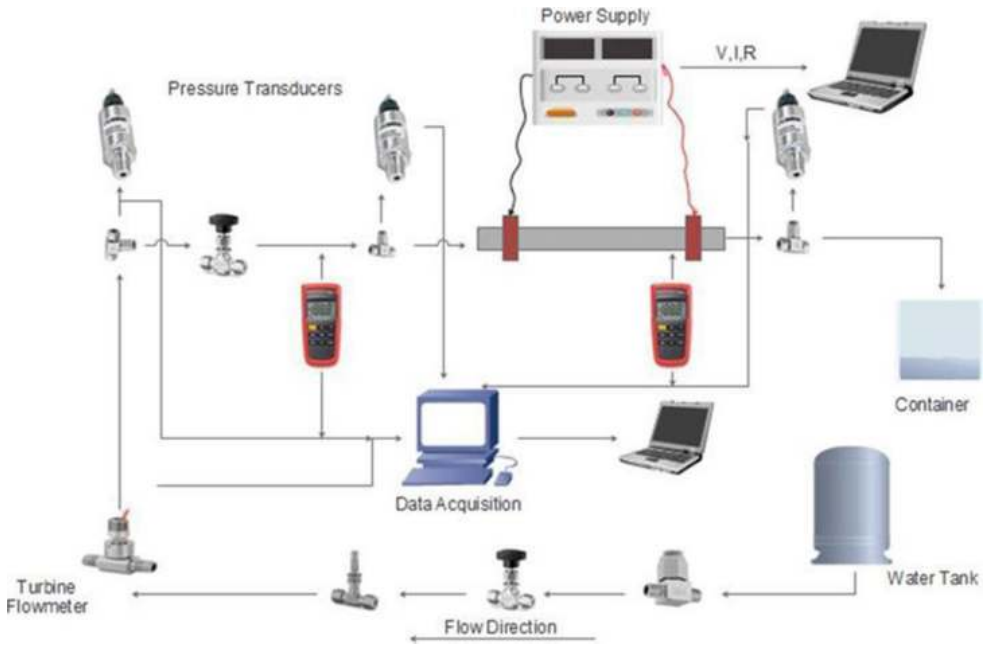

FIG. 6. Schematic of the experimental setup.

III. DATA REDUCTION AND UNCERTAINTIES

The collected voltage, current, flow rate, and temperature data are acquired via the Data Acquisition System in order to obtain single-phase and two-phase heat transfer coefficients.

The mass flux is defined as:

$$G = \dot{m}/A_c \tag{1}$$

where $\dot{m}$ is the mass flow rate and A_c is the cross section area of the microtube. The applied heat flux can be found using the microtube inner diameter and net applied power formula:

$$q'' = \frac{(P - \dot{Q}_{loss})}{\pi d_i L_h} \tag{2}$$

where d_i is the inner diameter of the microtube, L_h is the heated length, and $\left(P - \dot{Q}_{loss}\right)$ is the applied net power. The heat transfer coefficient at the exit of the tube is expressed as:

$$h_{tp} = \frac{(P - \dot{Q}_{loss})}{\pi d_i L_h (T_{w,\,i} - T_f)} \tag{3}$$

where $T_{w,i}$ is the local inner surface temperature and T_{fluid} is the local bulk fluid temperature at that location. $T_{w,i}$ is calculated using the measured local outer surface temperature,$T_{w,o}$ and assuming 1D steady state heat conduction with uniform heat generation as follows:

$$T_{w,i} = T_{w,o} + \frac{\dot{q}}{4k_w}\left({r_o}^2 - {r_i}^2\right) - \frac{\dot{q}}{2k_w}{r_o}^2 \log\left(\frac{r_o}{r_i}\right) \tag{4}$$

where r_i and r_o are the inner and outer radii of the microtube, respectively, k_w is the heat thermal conductivity of the wall, and $\dot{q}$ is the volumetric heat generation expressed in terms of the net power as:

$$\dot{q} = \frac{(P - \dot{Q}_{loss})}{\pi\,({r_o}^2 - {r_i}^2)\,L_h} \tag{5}$$

The local bulk fluid temperature is found through energy balance as:

$$T_f = T_i + \left[\frac{(P - \dot{Q}_{loss})x_{th}}{\dot{m}c_p L_h}\right] \tag{6}$$

where $\dot{m}$ is the mass flow rate, c_p is specific heat,T_i is inlet temperature, x_{th} is the thermocouple location, and L_h is the heated length of the microchannel.

The uncertainties in the measured values are given in Table I. They are based on the data in the manufacturer's datasheets and the propagation of uncertainty method.[44]

IV. RESULTS AND DISCUSSION

A. Single Phase Validation

Before performing systematic boiling heat transfer experiments on the coated surfaces, single phase tests were performed on plain microtubes in order to check for the validity of the experimental setup. Figure 7 demonstrates experimental results for the plain surface microtube at the

TABLE I. Uncertainties in experimental parameters.

Parameter	*Error*
Inner diameter, d_i	±2 μm
Electrical power, P	±0.17%
Heat flux, q''	±3.4%
Two phase heat transfer coefficient, h_{tp}	±11.8%
Inlet fluid temperature, T	±0.1°C
Mass flux, G	±2.5%

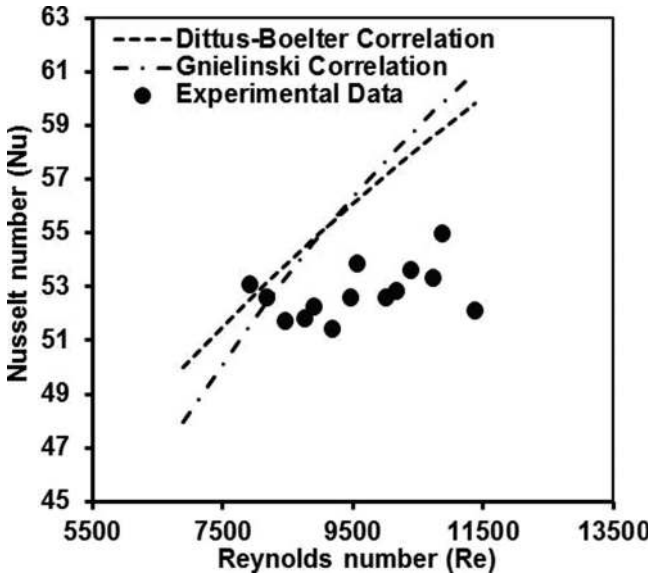

FIG. 7. Experimental single-phase heat transfer results in comparison with the existing correlations.

mass flux of 9500 kg/m^{2}s. Since turbulent flow conditions existed ($7000 < \mathrm{Re} < 11000$), the results were compared to the two well-known empirical correlations recommended for turbulent flows: Gnielinski and Dittus-Boelter correlations as shown in Eqs. (7) and (8), respectively:[45]

$$Nu = 0.023\, Re^{0.8}\, Pr^{0.4} \tag{7}$$

$$Nu = \frac{\left(\frac{f}{8}\right)(Re - 1000)\, Pr}{1 + 12.7\,(f/8)^{0.5}\,(Pr^{\frac{2}{3}} - 1)} \tag{8}$$

The following expression[42] was used to calculate f (friction factor) in Eq. (8):

$$f = (0.79\, lnRe - 1.69)^{-2} \tag{9}$$

A good agreement can be observed between the experimental results and the predictions of the two correlations. The maximum errors corresponding to Dittus-Boelter and Gnielinski correlations were about 12% and 15%, respectively. In this study, axial conduction effects were considered to be negligible due to high mass flux in this study that results in high Peclet number (ranged from about 30377 to 31974) which is defined as the product of the Reynolds number and the Prantdl number.[46,47]

B. Boiling curves

In order to investigate the effects of variations in wettability, experiments were conducted in two directions of the microtubes such that first the hydrophilic inlet (pHEMA coated inlet) and the hydrophobic outlet (pPFDA coated outlet) were considered. The tests were then repeated for the opposite case (pPFDA coated inlet and pHEMA coated outlet). Figure 8 displaying the boiling curves for the coated tubes at the mass flux of 9500 kg/m^{2}s illustrates that coated tubes result in a lower wall superheat at a fixed heat flux relative to the bare surface tube. Therefore, a shift to the left can be seen for the coated tubes, and the highest shift occurs in the microtube with the pHEMA coated (hydrophilic outlet) outlet. This is due to the decreased contact angle of the pHEMA coated side. Contact angle measurments reveal that the wettability varied from about 40 ° to about 110 ° when moving along the microtube from the pHEMA coated side to the pPFDA coated side. Therefore, higher heat fluxes could be sustained by the extra wetting layer on the inner walls of the microtube near the outlet.

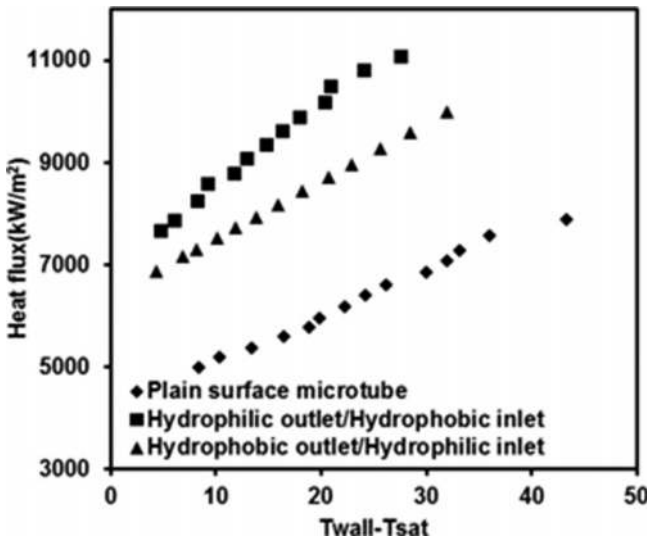

FIG. 8. Boiling curves corresponding to bare surface microtubes and gradient coated microtubes.

C. Heat Transfer Results

Figure 9 displays experimental boiling heat transfer coefficients as a function of heat flux. It is obvious from the figure that heat transfer is significantly enhanced with gradient pHEMA/pPFDA coatings. At high heat fluxes, heat transfer coefficients have higher values for all the experiments, which is associated with more nucleation at higher heat fluxes. Enhanced heat transfer in coated microtubes is due to the high porosity of the surface, which enables more nucleation and quicker bubble release from the surface. For the pHEMA coated inlet and pPFDA coated outlet (hydrophilic outlet and hydrophobic inlet), this effect is more dominant near the inlet of the heated section, while it is more pronounced toward the outlet for the hydrophobic outlet (pPFDA coated outlet, pHEMA coated inlet). The configuration with the pHEMA coated outlet benefits from the more hydrophilic surface near the outlet, where the surface temperature is expected to be the highest. This location is therefore more critical for the formation of dry spots, which badly influence heat transfer. More wettability toward the outlet facilitates rewetting of the surface thereby avoiding deterioration in

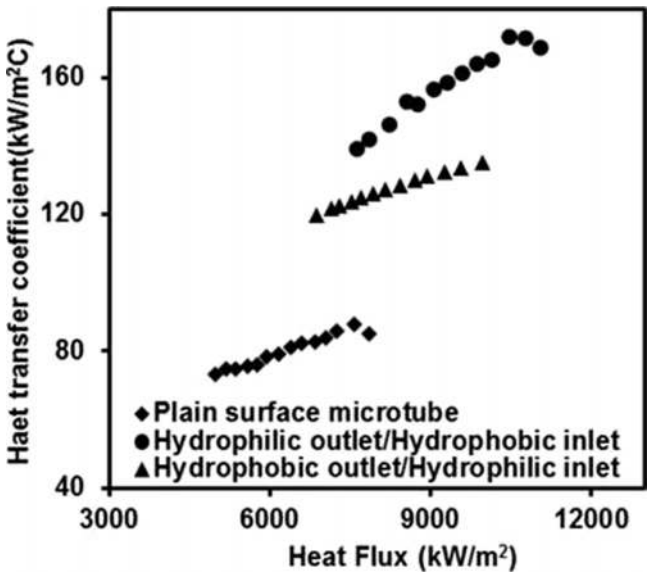

FIG. 9. Boiling heat transfer coefficients as a function of heat flux.

heat transfer. For the configuration with the pPFDA coated outlet and pHEMA coated inlet (hydrophobic outlet, hydrophilic inlet), the locations near the outlet are more hydrophobic. At these critical locations, rewetting becomes more difficult. As a result, dry spots are more likely to appear on the surface for these coatings, which results in a worse performance than the case with the hydrophilic outlet and hydrophobic inlet.

Another feature of the coatings is offering variations in wettability along the microtube. The existence of wettability gradient mitigates liquid motion and bubble motion near the surface thereby enhancing convective heat transfer. Positive effects of wettability gradient were also documented in the literature on heat and mass transfer in micro scale.[48–50] Figure 10 shows enhancements in boiling heat transfer coefficients for microtubes with hydrophilic outlet/hydrophobic inlet, hydrophobic outlet/hydrophilic inlet coatings, which were compared to the results from the microtubes uniformly coated with pHEMA in the study of Kaya et al.[29] As can be seen from the figure, the maximum heat transfer enhancement ratios were about 64% and 47% for the configurations with the pHEMA and pPFDA coated outlets (hydrophilic outlet/hydrophobic inlet and hydrophobic outlet/hydrophilic inlet), respectively. In the study of Kaya et al.,[29] the authors reported a maximum enhancement of 26% with only pHEMA coated microtubes (hydrophilic) under similar conditions with the present study. Higher enhancements in this study compared to the previous study of Kaya et al.[29] reveal the advantageous effects of variations in wettability with pHEMA/pPFDA coated microtubes on heat transfer enhancement. Due to the hydrophilic nature of pHEMA coatings, some potential nucleation sites are occupied by the liquid phase particularly near the inlet. The coating in the present study, however, promotes nucleation near the inlet and rewetting near the outlet, which leads to an increase in the boiling heat transfer performance relative to the pHEMA coating. Moreover, mitigation of the bubble motion and enhanced convective effects with the variation in wettability further contribute to the performance. Using pHEMA/pPFDA coated microtubes instead of only hydrophobic coated microtubes (only pPFDA coated microtubes) results in a decrease in dry spots, which typically appear near the exit of the microtube and might trigger a rise in the surface temperature at high heat fluxes for hydrophobic surfaces."

The experimental results obtained in this study revealed that the use of pHEMA and pPFDA coatings, which provide variations in wettability along the channel, could be a viable alternative for a superior boiling heat transfer performance. However, more studies are needed to investigate different parameters of these types of coatings to optimize the heat transfer performance of such enhancement techniques.

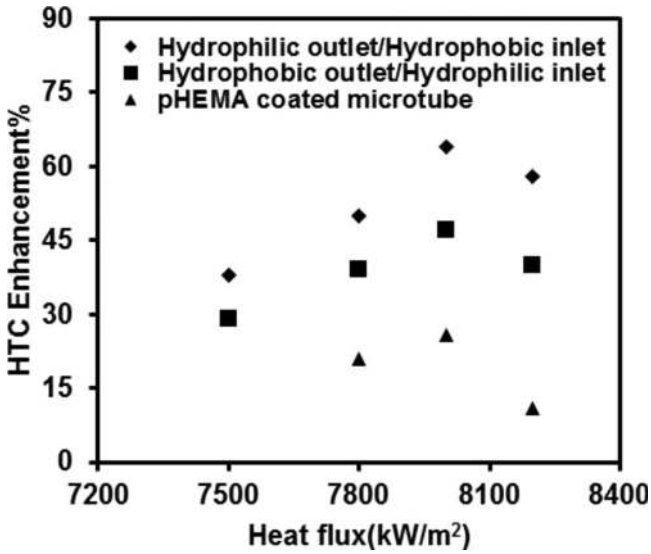

FIG. 10. Boiling heat transfer enhancement ratio as a function of heat flux for hydrophophilic outlet/inlet-hydrophobic inlet/outlet microtube configurations along with the results of the pHEMA coated microtubes in the study of Kaya et al.[29] for microtubes having inner diameters of 502 μm and mass flux of 9500 kg/m^2s.

V. CONCLUSIONS

Subcooled flow boiling heat transfer was investigated in microtubes with gradient poly hydroxyethyl methacrylate (pHEMA) and poly perfluorodecylacrylate (pPFDA) coatings, which offered variations in wettability along the microtube (increase and decrease toward the outlet, respectively). The main findings of the current study are as follows:

1. Gradient pHEMA/pPFDA coated microtubes offered superior boiling heat transfer performances in comparison to the plain surface microtube due to more active nucleation sites which yields in higher nucleation site densities, bubble generation frequency of the surface, as well as enhanced convective effects with the variation in wettability and improved liquid replenishment after bubble departure.
2. The best heat transfer coefficients corresponded to the configuration with the hydrophilic outlet and hydrophobic inlet (pHEMA coated outlet, pPFDA coated inlet) due to the higher wettability at critical locations and more active nucleation sites near the inlet. The maximum enhancement ratio in this configuration was ~64% while it was ~47% for the configuration with the hydrophilic inlet and hydrophobic outlet (pHEMA coated inlet, pPFDA coated outlet) at the same heat flux.
3. iCVD method was utilized for coating the inner walls of the microtubes. The results revealed that iCVD is an advantageous technique for having functional coatings on microchannel/tube surfaces with closed cross section geometries, where the application of existing conventional fabrication methods is limited.

ACKNOWLEDGMENT

The authors would like to thank the Sabanci University Nanotechnology Research and Application Center (SUNUM) for the continued equipment and characterization support. This work was supported by Turkish Scientific Council, Grant No. 115M365. Graduate student support provided by the faculty of Engineering and Natural Sciences of Sabanci University is greatly appreciated.

NOMENCLATURE

A_c = cross-sectional area, (m^2)
c_p = specific heat of water, (kJ/kg K)
d = channel diameter, (m)
f = friction factor, (-)
G = mass flux, (kg/m^2s)
h = heat transfer coefficient, (W/m^2K)
k = heat thermal conductivity, (W/m K)
L = length, (m)
$\dot{m}$ = mass flow rate, (kg/s)
Nu = Nusselt number, (-)
Pr = Prandtl number, (-)
P = electrical power, (W)
q'' = heat flux, (W/m^2)
$\dot{q}$ = volumetric heat generation, (W/m^3)
$\dot{Q}_{loss}$ = heat loss, (W)
r = radius, (m)
Re = Reynolds number, (-)
T = temperature, (°C)
x_{th} = thermocouple location, (m)

Subscripts

f = fluid
h = heated

i = inlet, inner
o = outer
w = wall

[1] J.C. Chen, *Convective Flow Boiling* (CRC Press, 1996).
[2] J.L. Cohen, D. a. Westly, A. Pechenik, and H.D. Abruña, J. Power Sources **139**, 96 (2005).
[3] R.S. Jayashree, S.K. Yoon, F.R. Brushett, P.O. Lopez-Montesinos, D. Natarajan, L.J. Markoski, and P.J. a. Kenis, J. Power Sources **195**, 3569 (2010).
[4] S.A. Mousavi Shaegh, N.-T. Nguyen, and S.H. Chan, Int. J. Hydrogen Energy **36**, 5675 (2011).
[5] L.S. Tong and Y.S. Tang, *Boiling Heat Transfer And Two-Phase Flow* (CRC Press, 1997).
[6] N-T Nguyen and S T Wereley, *Fundamentals and Applications of Microfluidics*, Second ed. (MA: Artech House Publishers, Norwood, 2006).
[7] D.J. Beebe, G.A. Mensing, and G.M. Walker, Annu. Rev. Biomed. Eng. **4**, 261 (2002).
[8] B. Ziaie, Adv. Drug Deliv. Rev. **56**, 145 (2004).
[9] A. Koşar, C.-J. Kuo, and Y. Peles, J. Heat Transfer **127**, 1106 (2005).
[10] B. Schneider, A. Koşar, C.-J. Kuo, C. Mishra, G.S. Cole, R.P. Scaringe, and Y. Peles, J. Heat Transfer **128**, 1293 (2006).
[11] B. Schneider, A. Koşar, and Y. Peles, Int. J. Heat Mass Transf. **50**, 2838 (2007).
[12] A. Koşar, C.-J. Kuo, and Y. Peles, Int. J. Heat Mass Transf. **48**, 4867 (2005).
[13] C.-J. Kuo and Y. Peles, Int. J. Heat Mass Transf. **50**, 4513 (2007).
[14] M. Shojaeian and A. Koşar, Exp. Therm. Fluid Sci. **63**, 45 (2015).
[15] W. Frost and C.J. Kippenhan, Int. J. Heat Mass Transf. **10**, 931 (1967).
[16] M. Gulliksen, H. Haugerud, and H. Kristiansen, Proc. 5th ASME/JSME Jt. Therm. Eng. Conf. 15 (1999).
[17] D.S. Wen and B.X. Wang, Int. J. Heat Mass Transf. **45**, 1739 (2002).
[18] M.S. Sarwar, Y.H. Jeong, and S.H. Chang, Int. J. Heat Mass Transf. **50**, 3649 (2007).
[19] H.T. Phan, N. Caney, P. Marty, S. Colasson, and J. Gavillet, Int. J. Heat Mass Transf. **52**, 5459 (2009).
[20] H. Trieu Phan, N. Caney, P. Marty, S. Colasson, and J. Gavillet, J. Heat Transfer **134**, 020901 (2012).
[21] V. Khanikar, I. Mudawar, and T. Fisher, Int. J. Heat Mass Transf. **52**, 3805 (2009).
[22] C.S. Sujith Kumar, S. Suresh, L. Yang, Q. Yang, and S. Aravind, Appl. Therm. Eng. **65**, 166 (2014).
[23] E. Forrest, E. Williamson, and J. Buongiorno, Int. J. Heat Mass Transf. **53.1**, 58 (2010).
[24] W. Wu, H. Bostanci, L.C. Chow, Y. Hong, M. Su, and J.P. Kizito, Int. J. Heat Mass Transf. **53**, 1773 (2010).
[25] S. Krishnamurthy and Y. Peles, J. Heat Transfer **132**, 041007 (2010).
[26] B. Stutz, C.H.S. Morceli, M.D.F. da Silva, S. Cioulachtjian, and J. Bonjour, Exp. Therm. Fluid Sci. **35**, 1239 (2011).
[27] H. Jo, H.S. Ahn, S. Kang, and M.H. Kim, Int. J. Heat Mass Transf. **54**, 5643 (2011).
[28] a. K.M.M. Morshed, F. Yang, M. Yakut Ali, J. a. Khan, and C. Li, Appl. Therm. Eng. **32**, 68 (2012).
[29] A. Kaya, R. Demiryürek, E. Armağan, G. Ozaydin-Ince, M. Sezen, and A. Koşar, J. Micromechanics Microengineering **23**, 115017 (2013).
[30] T. Çikim, E. Armagan, G. Ozaydin Ince, and A. Kosar, J. Heat Transfer **136**, 081504 (2014).
[31] A.K.M.M. Morshed, T.C. Paul, and J. a. Khan, Exp. Therm. Fluid Sci. **47**, 6 (2013).
[32] A.K.M.M. Morshed, T.C. Paul, and J. Khan, Appl. Therm. Eng. **51**, 1135 (2013).
[33] X. Ji, J. Xu, Z. Zhao, and W. Yang, Exp. Therm. Fluid Sci. **48**, 198 (2013).
[34] A.R. Betz, J. Jenkins, C.J. Kim, and D. Attinger, Int. J. Heat Mass Transf. **57**, 733 (2013).
[35] P. Bai, T. Tang, and B. Tang, Appl. Therm. Eng. **58**, 291 (2013).
[36] S. Kumar, S. Suresh, C.R. Aneesh, S. Kumar, A.S. Parveen, and K. Raji, Appl. Surf. Sci. **334**, 102 (2015).
[37] W.E. Tenhaeff and K.K. Gleason, Adv. Funct. Mater. **18**, 979 (2008).
[38] G. Ozaydin-Ince and K.K. Gleason, J. Vac. Sci. Technol. A Vacuum, Surfaces, Film. **27**, 1135 (2009).
[39] M.E. Alf, A. Asatekin, M.C. Barr, S.H. Baxamusa, H. Chelawat, G. Ozaydin-Ince, C.D. Petruczok, R. Sreenivasan, W.E. Tenhaeff, N.J. Trujillo, S. Vaddiraju, J. Xu, and K.K. Gleason, Adv. Mater. **22**, 1993 (2010).
[40] K.K.S. Lau and K.K. Gleason, Macromolecules **39**, 3695 (2006).
[41] P. Larkin, *Infrared and Raman Spectroscopy; Principles and Spectral Interpretation* (Elsevier, 2011).
[42] K. Chan and K.K. Gleason, Langmuir **21**, 8930 (2005).
[43] M. Gupta and K.K. Gleason, Langmuir **22**, 10047 (2006).
[44] S. Kline and F. McClintock, Mech. Eng. (1953).
[45] F. Incropera and D. Dewitt, (1985).
[46] K.D. Cole and B. Çetin, Int. J. Heat Mass Transf. **54**, 2542 (2011).
[47] G.L. Morini, Heat Transf. Eng. **27**, 64 (2006).
[48] M. Kaviany, Springer Sci. Bus. Media (2012).
[49] S. Daniel, M.K. Chaudhury, and J.C. Chen, Science **291**, 633 (2001).
[50] M.K. Chaudhury and G.M. Whitesides, Science **256**, 1539 (1992).